Infrared and Raman Studies on Films of Organosiloxane Networks Produced by PECVD

B. C. Trasferetti† and C. U. Davanzo*

Instituto de Química, Universidade Estadual de Campinas, Caixa Postal 6154, CEP-13.083-970, Campinas-SP, Brazil

M. A. Bica de Moraes

Instituto de Física "Gleb Wataglin", Universidade Estadual de Campinas, Caixa Postal 6165, CEP-13.087-970, Campinas-SP, Brazil

Received September 3, 2003; Revised Manuscript Received November 3, 2003

ABSTRACT: The effect of the incorporation of oxygen and nitrogen on the structure of films obtained by PECVD of hexamethyldisiloxane (HMDSO)−He−N_2 and HMDSO−He−O_2 mixtures is investigated using infrared and Raman spectroscopies. From transmittance spectra of films deposited onto single-crystal KBr disks, the transverse optical (TO) and longitudinal optical (LO) functions in the mid-infrared region were calculated. To correlate structural aspects with the observed LO−TO splittings, an identification analysis of functional group based on the infrared and Raman literature was made. It was concluded that the structure of the films deposited from HMDSO−He−O_2 discharges was strongly dependent on the proportion of oxygen in the gas feed. In the absence of oxygen, i.e., for a discharge of a HMDSO−He mixture, the resulting film consisted of a network of interconnected siloxane and carbosilane units. Addition of O_2 precluded the formation of methylene bridges and induced the formation of a material enriched with Si−O−Si groups. Films formed from the HMDSO−He−N_2 plasmas, on the other hand, consisted mainly of interconnected siloxane and carbosilane units in addition to a small quantity of silazane units. On the basis of these results, we propose an interpretation for the variation of the LO−TO splitting amplitude for the asymmetrical stretching mode (AS1) of Si−O in Si−O−Si groups as a function of the oxygen or nitrogen incorporation into the films.

Introduction

Organosiloxane films produced by plasma-enhanced chemical vapor deposition (PECVD) have been widely investigated as candidates for a large variety of applications. These comprise biocompatible coatings for medical implants,[1] permselective membranes,[2] oxygen barrier coatings on polymers for the packaging industry,[3] and low dielectric constant interlevel dielectrics in microcircuits.[4] This ample range of prospective applications is due to the unique properties of these materials, such as chemical inertness, hardness, thermal stability, insolubility, coherency, and adherence to several types of substrates.[1−12] Furthermore, as most materials synthesized by PECVD, organosilicone films may form uniform films on substrates with complex topologies. For the production of organosilicone films by PECVD, several monomers have been used, including those not polymerizable by conventional means. However, recently, organosilicones such as hexamethyldisiloxane (HMDSO) began to replace the often used, but hazardous monomers such as silane, which is pyrophoric. Furthermore, HMDSO has the added advantages of lower cost relative to silane and tetraethoxysilane (TEOS) and a higher room temperature vapor pressure (48 Torr) than TEOS (4 Torr).[9]

This work presents an investigation on the structure of thin films deposited from plasmas of HMDSO−He−O_2 and HMDSO−He−N_2 mixtures. A number of studies carried out in films deposited from plasmas of HMDSO mixed with other gases have shown that they strongly influence film structure and composition. Highly reactive oxygen and nitrogen species were formed from the addition of O_2 or N_2 to the plasma, resulting in the incorporation of these elements into the films. Furthermore, the atomic oxygen species react with carbon, forming volatile CO and CO_2 species and thus reducing the amount of carbon incorporated into the film. While the physical properties of films of low carbon content approach those of silicon oxide, nitrogen-containing organosilicone films may find useful applications. It has been reported that silicon nitrided oxides suppress the dopant diffusion across the oxide−silicon interface, and since their electrical properties are essentially as good as those of conventional oxides, they are particularly suited for dielectric gates.[13,14] Another important structural issue concerning these films is whether and in which conditions the incorporation of Si−CH_2−Si groups take place. The partial replacement of the oxygen atoms of a pure silica network by methylene groups has generated materials exhibiting good insulating and thermal properties, such as high thermal stability and high thermal conductivity.[15−17]

In the present work, film characterization was carried out by vibrational spectroscopy. For the infrared characterization, a recently reported approach employed to investigate films deposited from discharges of tetramethylsilane−Ar−O_2 mixtures was used.[18] It consists of the determination of the dielectric functions of the samples by means of Kramers−Krönig analysis of their transmittance spectra. Such an approach allows the assessment of both longitudinal (LO) and transverse

† Present address: Instituto de Física "Gleb Wataglin", Universidade Estadual de Campinas, Caixa Postal 6165, CEP-13.087-970, Campinas-SP, Brazil.

* Corresponding author: e-mail celso@iqm.unicamp.br.

10.1021/ma035297a CCC: $27.50
Published on Web 12/18/2003

Table 1. Flow Rates Used for Film Deposition, Film Thickness, and Refractive Index[a]

sample	F_{O_2} (sccm)	F_{He} (sccm)	F_{N_2} (sccm)	d (μm)	n ($\lambda = 633$ nm)
He100	0	100	0	1.15	1.49
O50	50	50	0	1.50	1.48
O100	100	0	0	1.16	1.43
N50	0	50	50	0.60	1.53
N100	0	0	100	0.50	1.60

[a] F_{O_2}, F_{N_2}, and F_{He} are flow rates of O_2, N_2, and He; d and n are the film thickness and refractive index, respectively.

(TO) optical functions.[19,20] Raman spectroscopy was another important characterization technique used here. Though some work has been reported[21−23] in characterizing pure organosilicon molecules using Raman spectroscopy, little has been reported on the use of this technique to characterize films produced by PECVD, and therefore, our results can be used as a reference in future applications of Raman spectroscopy to characterize siloxane networks.

Experimental Section

The reactor employed for the PECVD synthesis is a radio-frequency reactor that has been described in our previous paper.[18] All depositions were carried out at the HMDSO partial pressure of 2.5 Pa and the radio-frequency power of 50 W. The O_2, N_2, and He flow rates used to deposit the various films are listed in Table 1. The samples were labeled according to the gas mixture used in their preparation. As substrates, we have used single-crystal KBr disks and aluminum-coated glass slides. Table 1 also lists the film thickness, obtained with a high-resolution profilemeter (Dektak 3) and the index of refraction at $\lambda = 632.8$ nm, determined using the Abeles method.[24]

The infrared spectra were obtained for all samples in a Bomen MB-101 FT-IR spectrometer equipped with a DTGS detector. The spectral range covered was 400−5000 cm^{-1}. Each spectrum was the result of co-adding 64 scans collected at 4 cm^{-1} resolution. The transmission and reflection−absorption spectra were obtained from films deposited on KBr disks and aluminum-coated glass slides, respectively. For the reflection−absorption measurements, a variable-angle attachment (SPECAC) was used. The incidence angle was 70° off-normal, and the incident beam was p-polarized. Polarization was provided by the insertion of a grid polarizer (SPECAC) in the optical path. All reflection−absorption measurements were referenced to an aluminum mirror, whereas the transmission ones were referenced to a bare KBr disk.

Raman spectra of the films supported on Al-coated glass were acquired in a Jobin Yvon T64000 spectrometer attached to a microscope. An Ar^+ laser at $\lambda = 514.5$ nm and 100 mW output power was used for excitation. Both the Raman and the infrared spectra were taken at room temperature.

The infrared data analysis used here has been described elsewhere.[18] In brief, the determination of the optical constants (refractive and absorption indices, n and k, respectively) was performed using the Kramers−Krönig analysis (KKA) of transmission data.[25] From the absorption spectrum of a film of known thickness deposited on a transparent KBr disk, $k(\lambda)$ is determined. From $k(\lambda)$ and the value of n_∞ (the refraction index of the material in the visible range), $n(\lambda)$ can be determined by means of the KKA. The calculations were carried out following a previously described algorithm.[26]

Once the $n(\lambda)$ and $k(\lambda)$ functions are obtained, the complex dielectric function $\tilde{\epsilon} = (n + ik)^2$ can be calculated. Finally, the TO and LO functions, whose maxima correspond to the vibrational modes TO and LO, respectively, can be determined from the following equations:[27]

$$\text{TO function} = \text{Im}(\tilde{\epsilon})$$

$$\text{LO function} = \text{Im}(-1/\tilde{\epsilon})$$

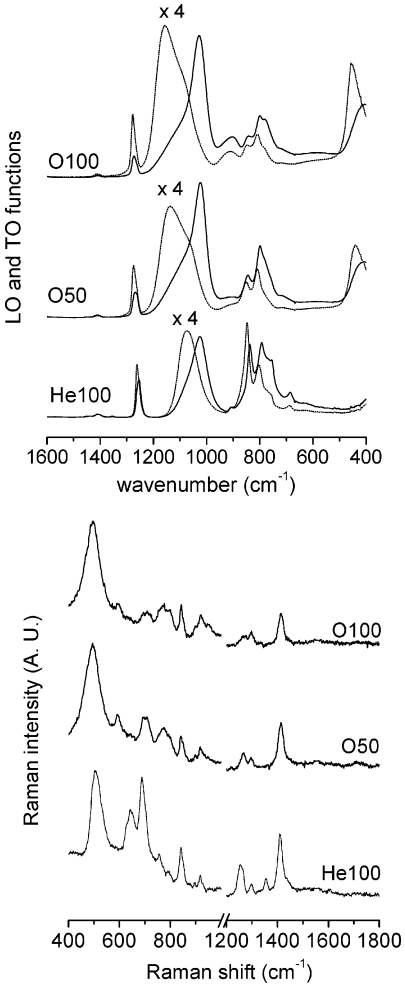

Figure 1. LO (dotted lines) and TO (full lines) functions in the infrared low-frequency region (top) and Raman spectra of the samples in the O group (bottom).

To check the quality of the retrieved optical constants, a test outlined in our previous paper was performed.[18] In brief, it consists of simulating reflection−absorption spectra of a thin film deposited on aluminum taken at an incidence of 70°, using p-polarized light and comparing them with experimental ones. The simulation is carried out through the Fresnel equation for a three-phase layered system.[27]

Results

Spectral Data and Chemical Groups Forming the Solid Films. Samples were divided into two groups: the O and the N group. Films deposited from plasmas of HMDSO−He−O_2 and HMDSO−He−N_2 mixtures belong to the O and the N group, respectively. The sample deposited from the HMDSO−He mixture was added to both groups and is considered to be their baseline to investigate the effects of O_2 and N_2 dilution.

LO and TO functions in the low-frequency region and Raman spectra for samples of the O group are shown in Figure 1 while those for the samples of the N group are shown in Figure 2. Figure 3 exhibits TO functions of all samples in the high-frequency region. Only the TO functions are shown in this figure because LO and TO functions are nearly superimposed in the frequency range presented.

Band assignments for both IR and Raman bands were made according to theoretical and experimental studies on model silicon-containing molecules.[21−23,28−31] Tables 2 and 3 summarize the assignments of the main

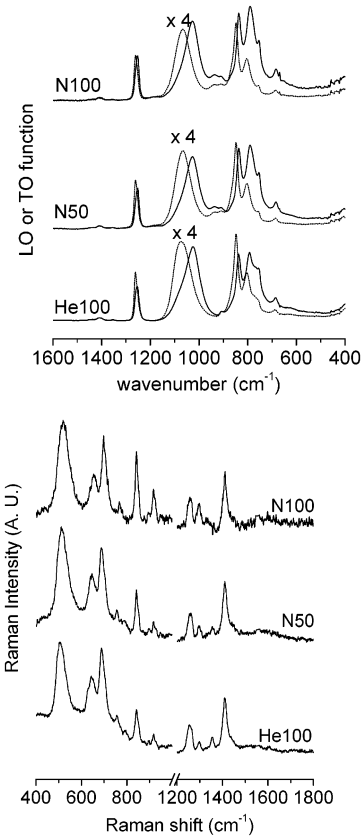

Figure 2. LO (dotted lines) and TO (full lines) functions in the infrared low-frequency region (top) and Raman spectra of the samples in the N group (bottom).

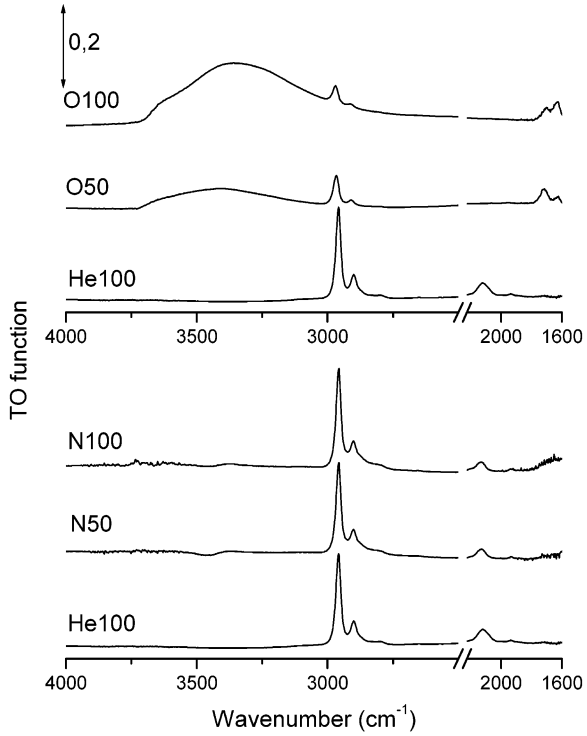

Figure 3. TO functions in the high-frequency region for all the samples deposited on KBr.

observed bands in the IR and Raman spectra, respectively. In the case of Raman spectra, three low-intensity bands could not be assigned, as indicated in Table 3.

To make assignments for the IR bands, only TO modes were considered since all the literature available on this subject is based on transmission measurements taken at normal incidence, with which only TO modes can be detected. A detailed discussion on the observed chemical groups of the deposited films is presented below:

Si−O Groups. In Figures 1 and 2, both TO and Raman spectra exhibited clear-cut bands related to Si−O−Si groups: at ∼1030 cm^{-1} in the IR spectra and at ∼500 cm^{-1} in the Raman spectra. The IR bands at ∼1030 cm^{-1} are attributed to the asymmetrical stretching mode of Si−O−Si groups and lie at a frequency range that is characteristic of a suboxide configuration[7] or a polymeric siloxane.[8] These bands are termed AS1 in analogy to the nomenclature currently used for the same mode in vitreous SiO_2 (v-SiO_2).[18,33] The variation of the AS1 band position was small: it lied between 1024 and 1034 cm^{-1} for all samples.

The Raman band at ∼500 cm^{-1} is attributed to the Si−O symmetrical stretching (SS) mode in Si−O−Si groups.[28] For thermal SiO_2, it lies at 810 cm^{-1} and is a weak IR band.[33] Actually, both its Raman or IR activity and position are known to be strongly related to the intertetrahedral Si−O−Si bond angle. In our case, we have to consider the fact that our films have a high amount of methyl groups, and therefore, the SS mode may be influenced by their presence. The presence of methyl groups allows the Si−O−Si bond angle to assume values that are higher than that of v-SiO_2, for which this bond angle averages about 134° according to recent theoretical studies.[34] For silsesquioxanes containing organic side groups, Calzaferri and co-workers[35,36] have shown that the Si−O−Si bond angle vary from 144° to 153°. Recent theoretical studies carried out by McKean[28] indicate that for the HMDSO molecule the SS mode is not IR-active, and the most stable molecular configuration was attained when the Si−O−Si bond angle was 149°. These pieces of information suggest that the absence of the SS-mode-related band in the IR spetra and its position in the Raman spectra (very close to that observed for the HMDSO molecule[28]) can be explained by an average intertrahedral angle higher than that calculated for v-SiO_2 and closer to those observed for silsesquioxane structures and for the HMDSO molecule.

For samples O50 and O100, the Raman spectra exhibit a low-intensity band at 595 cm^{-1}, which, according to Gleason and co-workers,[37] can be attributed to an organically substituted ring consisting of three siloxane units, bound to the siloxane network.

$Si(CH_3)_x$ Groups. Several bands related to methyl groups bonded to silicon atoms are present in the TO and Raman spectra of Figures 1 and 2. In the IR spectra, the most obvious one is the asymmetrical deformation of methyl groups in $Si(CH_3)_x$ groups. For sample He100 and those of the N group it lied invariably at 1252 cm^{-1}. However, for samples of the O group, this band blue-shifted up to 1272 cm^{-1}. As pointed out in our previous work,[18] this band is sensitive to the presence of electronegative atoms such as oxygen bonded to the same silicon atom to which the methyl group is bonded. We also observed in the IR spectra of all samples a very low-intensity band at 1400 cm^{-1}, which is attributed to the symmetrical deformation of methyl groups in $Si(CH_3)_x$.[30] Both these symmetrical and asymmetrical deformations are also Raman-active and appear in the spectrum of Figures 1 and 2 at frequencies in the interval between 1254 and 1273 cm^{-1} for the sym-

Table 2. Wavenumber of Bands in the TO and LO Spectra of Films Deposited on KBr[a]

band position (cm^{-1})											
He100		O50		O100		N50		N100			
TO	LO	TO	LO	TO	LO	TO	LO	TO	LO	assignment[b]	ref
			443		455					ρ_{Si-O} in Si−O−Si	30
683	683					683	683	683	683	$\nu_{S,Si-C3}$	29
				780						ρ_{Me},ν_{SiC} in $Si-Me_1$	30
754						754		754		ρ_{Me},ν_{SiC} in $Si-Me_3$	30
793	803	800	809	800	809	790	803	790	806	ρ_{Me},ν_{SiC} in $Si-Me_2$	30
838	848	844	851	844	848	835	848	838	848	ρ_{Me},ν_{SiC} in $Si-Me_3$	30
908	908			904	908	908	908	908	908	$\nu_{AS,SiO}$ in Si−O−H	30
						934	934	937	937	$\nu_{AS,SiN}$ in Si−N−Si	21
1024	1075	1024	1137	1034	1160	1027	1066	1027	1066	$\nu_{AS,SiO}$ in Si−O−Si	30
1252	1262	1268	1275	1272	1278	1252	1262	1252	1262	$\delta_{S,Me}$ in $Si-Me_x$	30
1354	1354					1355	1355	1355	1355	γ_{CH_2} in $Si-CH_2-Si$	23
1410	1410	1411	1411	1411	1411	1410	1410	1410	1410	$\delta_{AS,Me}$ in $Si-Me_x$	30
		1619	1619	1626	1626					$\nu_{C=O}$	32
		1714	1714	1699	1699					$\nu_{C=O}$	32
2123	2123					2125	2125	2130	2130	ν_{Si-H}	30
2900	2900	2911	2911	2911	2911	2901	2901	2903	2903	$\nu_{S,C-H}$ in $Si-Me_x$	30
2958	2958	2963	2963	2970	2970	2957	2957	2956	2956	$\nu_{AS,C-H}$ in $Si-Me_x$	30

[a] Assignments are made from the literature for the TO modes. [b] ν, δ, ρ, and γ denote stretching, bending, rocking, and scissoring modes, respectively; AS and S denote asymmetric and symmetric vibrations.

Table 3. Raman Shift Wavenumbers for Films Deposited on Al-Coated Glass Substrates[a]

band position (cm^{-1})						
He100	O50	O100	N50	N100	assignment[b]	ref
508	494	494	511	519	$\nu_{S,SiO}$ in Si−O−Si	28
	595	596			$\nu_{S,SiO}$ in Si−O−Si	37
643			646	654	ρ_{Me},ν_{SiC} in $Si-Me_1$	30
688			688	698	ρ_{Me},ν_{SiC} in $Si-Me_3$	30
	709	709			$\nu_{S,SiC}$ in $Si-Me_2$	30
754			758	766	ρ_{Me},ν_{SiC} in $Si-Me_3$	30
	774	774			?	
	797	797			$\nu_{AS,SiC}$ in $Si-Me_2$	30
842	850	843	842	842	ρ_{Me},ν_{SiC} in $Si-Me_3$	30
919	918	921	918	917	?	
1254	1268	1273	1260	1257	$\delta_{S,Me}$ in $Si-Me_x$	30
1299	1296	1298	1296	1298	?	
1357			1355		γ_{CH2} in $Si-CH_2-Si$	30
1409	1414	1413	1410	1411	$\delta_{AS,Me}$ in $Si-Me_x$	30

[a] Assignments are made from the literature. [b] ν, δ, ρ, and γ denote stretching, bending, rocking, and scissoring modes, respectively; AS and S denote asymmetric and symmetric vibrations.

metrical mode and around 1410 cm^{-1} for the asymmetrical mode. However, in Raman spectra, the asymmetrical mode is more intense than the symmetrical one, as can be seen in Figures 1 and 2. It is important to remark that the band related to this symmetrical mode, at 1254 cm^{-1} in the He100 sample, also blue-shifted up to 1273 cm^{-1} for the O group samples.

In the 600−900 cm^{-1} range, we observed several bands that are related to Si−C stretchings and methyl rockings in $Si(CH_3)_x$ groups (cf. Tables 2 and 3) in both IR and Raman spectra. These bands are useful for characterizing the presence of monomethyl-, dimethyl-, and trimethyl-substituted silicon.[30] $Si-Me_3$ groups have three characteristic bands in both IR and Raman spectra: (i) at ∼685 cm^{-1}, (ii) at ∼755 cm^{-1}, and (iii) at ∼840 cm^{-1}. All of them are assigned both to methyl rockings and Si−C stretchings. All these bands appeared for samples in the N group. However, samples in the O group exhibited only the band at ∼840 cm^{-1}, which indicates that the amount of $SiMe_3$ groups is small in these samples. As for $Si-Me_2$ groups, we observed a characteristic band between 790 and 800 cm^{-1} in the IR spectra for all samples. However, Raman spectra showed this band only for samples O50 and O100. The other $Si-Me_2$-group-related Raman band at ∼710 cm^{-1} was also observed only for samples O50 and O100. Probably the high intensity of the band related to $Si-Me_3$ (at ∼688 cm^{-1}) overlaps them for the other samples. $Si-Me_1$-group-related bands were observed only for samples O50 and O100 (at ∼775 cm^{-1}) and both in the Raman and in the IR spectra.

As can be seen in Figure 3, the frequencies of the symmetrical and asymmetrical C−H stretchings in methyl groups (∼2900 and ∼2957 cm^{-1}, respectively, for sample He100 and those of the N group) are also very characteristic of methyl groups bonded to silicon.[30] For the O group samples, a small blue shift of these bands is observed with respect to those of the He100 sample.

An important information that can be drawn from the IR data shown in Figures 1 and 2 is that a significant amount of $Si(CH_3)_3$ groups are incorporated in the films deposited in the absence of oxygen. This is easily inferred if we consider the band at ∼680 cm^{-1}, which is related to $Si(CH_3)_3$ groups and is known to be very weakly IR-active,[21] and therefore its very observation is proof that a significant amount of $Si(CH_3)_3$ groups is present in the solid film. Since this group is a constitutive moiety of the precursor molecule, this is an indirect evidence that the degree of fragmentation is higher in the presence of oxygen.

Si−N and N−H Groups. Only IR spectroscopy accused the presence of Si−N bonds in samples of the N group through a band related to the asymmetrical stretching of Si−N groups.[21] There has been a recent discussion over the band position differences related to the local configuration of nitrogen atoms in silicon networks, i.e., whether it is connected to two or three silicon atoms.[38] The former configuration is supposed to give rise to a band in the 950−900 cm^{-1} range,[30] while the latter, which is the silicon nitride configuration, is expected at much lower frequencies (around 860 cm^{-1}). For samples N50 and N100, the band lied at ∼935 cm^{-1}, which is consistent with the presence of silazane moieties. This is confirmed through the observation of N−H stretching bands at around 3370 cm^{-1}, as shown in Figure 4.

$Si-CH_2-Si$ Groups. The formation of carbosilane moieties in samples He100, N50, and N100 was confirmed by the observation of a low-intensity IR (Figure

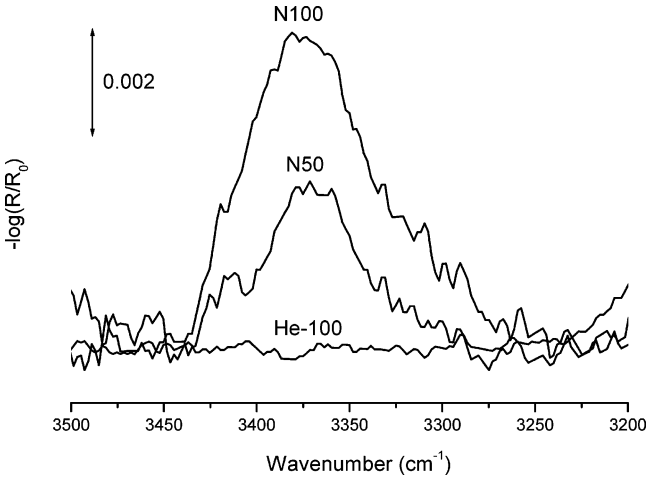

Figure 4. Reflection−absorption spectra in the N−H stretching region obtained for samples deposited on Al-coated glass slide.

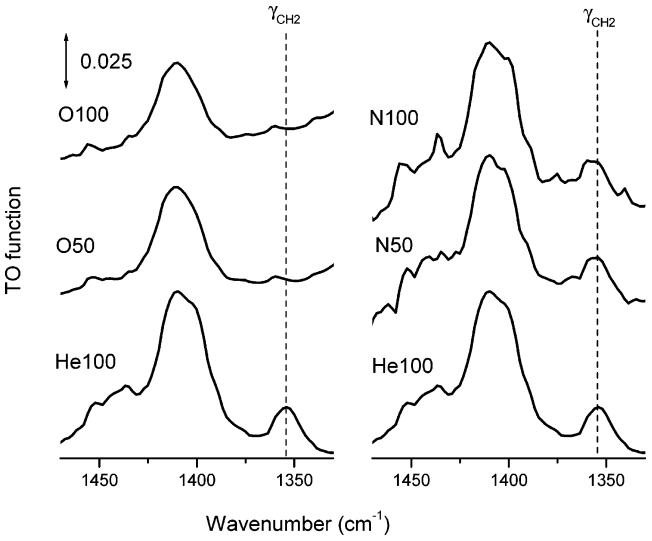

Figure 5. Magnified TO functions for all samples in the region of the scissoring of CH_2 in Si−CH_2−Si groups.

5) and Raman band at ∼1350 cm^{-1}. Such band is attributed to a scissoring mode of methylene (γ_{CH_2}) in Si−CH_2−Si groups.[23,39] Since it is very weakly active in the infrared, its very appearance in the spectra shows that the amount of these groups forming the solid film is significant. It is usually accompanied by the methylene wagging mode, which for the Si−CH_2−Si group lies at ∼1030 cm^{-1},[23,39] but it could not be observed in our spectra due to its proximity to the intense Si−O asymmetrical stretching mode. It is interesting to notice that the methylene scissoring band is not observed at all in the spectra of samples O50 and O100.

The Si−$(CH_2)_n$−Si group in silica-like structures (with $1 \leq n \leq 3$) has been recently investigated by Sugahara and co-workers.[15−17] For the film with $n = 1$, they did observe a band at ∼1360 cm^{-1}, which was attributed to the γ_{CH_2} in Si−(CH_2)−Si. It is important to stress that this band was not accompanied by the methylene C−H stretching bands. However, for films with $n = 2$, they have not observed the band at ∼1360 cm^{-1} and started to observe both the C−H stretchings and two bands at 1280 and 1160 cm^{-1}. The latter is related to Si−CH_2-CH_2−Si.[30] Therefore, it seems that the presence of successive methylene groups play an important role in the intensity and the position of CH_2-related bands.

Si−H Groups. A band at ∼2125 cm^{-1}, attributed to the Si−H stretching vibration, was observed in the IR spectra of samples He100, N50, and N100 (Figure 3). Since this mode is known to be strongly IR-active,[40] the low intensity of the observed bands indicates that the presence of these groups within these samples is only marginal.

Other Groups. The stretching of the carbonyl group was observed in the spectra of samples O50 and O100.[31] This shows that the incorporation of carbonyl groups is relevant only for films deposited from O_2-diluted HMDSO plasmas. We also observed the presence of sylanol groups, especially in samples O50 and O100.

Important exclusions were also made from the spectroscopic data. Raman spectroscopy provided very useful information: the spectra did not show any band that could be attributed to Si−Si bonds (a band related to Si−Si groups would be expected at ∼425 cm^{-1}).[37] Another general information is that the incorporation of methyl groups bonded to oxygen atoms was not observed (a very characteristic band related to this group should be observed at ∼2850 cm^{-1}).[41]

Film Structure. From the band assignments made above, we have built Table 4, containing several types of chemical units consisting of a central silicon atom bonded to bridging oxygen atoms or methylene groups or to network-terminating methyl groups. These units are thus distorted tetrahedra centered on silicon atoms and will be used in the discussion hereafter. The siloxane tetrahedra are labeled according to the conventional nomenclature used for silicon polymers; i.e., M, D, T, and Q represent silicon atoms with increasing number of oxygen substituents. We have also included in Table 4 tetrahedra containing methylene bridging units, which were labeled according to the following example: MCH_2 stands for a tetrahedra having one bridging oxygen and one bridging methylene unit. Note that Table 4 is not intended to be a rigorous summary of the silicon bonding environments present in our films, but it certainly describes the principal ones, disregarding the presence of traces of Si−H, C═O, and Si−OH groups. Tetrahedra having NH as bridging units, detected for samples deposited in the presence of N_2, were not included in Table 4 either because its incorporation is only marginal.

In general, the physical properties of all samples show evidence of intense cross-linking, since they are coherent, hard, and insoluble to common solvents such as propanol and acetone.

We have observed that, according to the deposition parameters, the bridging units between the silicon tetrahedra can be either oxygen or methylene or both of them. In cases in which both of the bridging units coexist, there is a certain difficulty with band assignment because the most intense band related to Si−CH_2−Si groups, the wagging of methylene groups in this chemical environment,[33] appears in a region very close to the strong asymmetrical stretching of Si−O in Si−O−Si groups. The differentiation can be made through a very weak band at ∼1350 cm^{-1}, which is attributed to the scissoring mode of methylene in Si−CH_2−Si groups,[8,23,33] as discussed above. Since this band is very weakly active in the IR, its very presence indicates significant amounts of this group in the film. The incorporation of methylene bridges only in samples He100, N50, and N100 is intriguing. To attempt to

Table 4. Possible Ending, Nonbranching, Branching, and Cross-Linking Nodes Present in PECVD Films[a]

Ending Nodes	Non-Braching Nodes	Crosslinking and/or Branching Nodes	
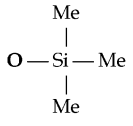	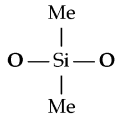	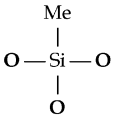	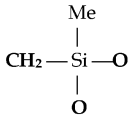
M	**D**	**T**	**DCH_2**
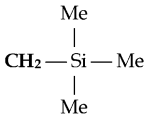	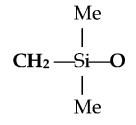	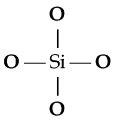	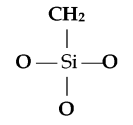
CH_2	**MCH_2**	**Q**	**TCH_2**

[a] Bridging groups are in boldface letters (for simplification, the 0.5 underscore was omitted in them).

Table 5. Structural Characteristics of the Samples

monomers and diluent gases	samples	types of tridimensional networks	possible distorted silicon tetrahedra
HMDSO, He	He100	organosiloxane and organocarbosilane	all those shown in Table 4
HMDSO, He, O_2	O50 and O100	organosiloxane	M, D, T, and Q
HMDSO, He, N_2	N50 and N100	organosiloxane, organocarbosilane, and organosilazane	all those shown in Table 4 plus a small amount of NH-bridging units

explain this observation, we have relied on recent studies of intermediate gas-phase precursors during PECVD of HMDSO.[3,42,43] According to them, two common fragmentation processes occurring in HMDSO plasmas are methyl and hydrogen abstraction. A methyl-abstracted HMDSO species presents a reactive silicon that can oligomerize by reaction with a hydrogen-abstracted HMDSO species. This mechanism would justify the incorporation of methylene bridges within the structure of samples He100, N50, and N100. However, for oxygen-diluted plasmas,[3] the prompt reaction between oxygen species and methylene from hydrogen-abstracted HMDSO species forming combustion gases may preclude the incorporation of CH_2 bridges.

The characteristics of the samples deposited according to the monomers and diluent gases are summarized in Table 5.

The films seem to be consisted of random networks containing no domains of a specific type of tetrahedrum. Otherwise, the different Si−O−Si group environments would give rise to band broadening and even to clear-cut band splittings. At this point, it is interesting to compare our results to those obtained by Gleason and co-workers for flexible siloxane films with a high polymeric character,[37,44] for which the AS1 mode splits into two resolved bands similar to poly(dimethylsiloxane). The difference between the spectra of our films and those obtained by Gleason and co-workers highlights the network character of our films.

It is known that a polymethylsiloxane polymer with a composition of 30% T and 70% D groups is a liquid at ambient conditions, and more cross-linked polymethylsiloxanes remain resinous up to a compostition of about 90% T and 10% D groups.[37] Therefore, although not straightforward from the spectral analysis, the presence of Q and/or TCH_2 groups in our samples is seemingly obvious due to the physical properties of the films (solidity and insolubility in common solvents) and due to the absence of evidence for the presence of Si−Si groups.

Table 6. LO−TO Splitting Amplitudes for Samples Deposited on KBr

sample	Δ_{LO-TO} (cm^{-1})	sample	Δ_{LO-TO} (cm^{-1})
He100	51	N50	39
O50	113	N100	39
O100	126		

LO−TO Splittings. The LO−TO splitting is an effect that has been observed for both amorphous and crystalline materials. In the area of amorphous materials, the LO−TO splitting for the AS1 mode in vitreous silica is well-documented[33,45−48] and can be interpreted as due to a strong long-range Coulombic interaction[49] between the Si−O−Si oscillators as a consequence of their high density in the films. However, with the exception of our previous work,[18] such splittings had not yet been observed in silicon-based networks.

Table 6 illustrates the AS1 mode LO−TO splitting amplitude (Δ_{LO-TO}) for the samples of the O and N groups. For samples of the O group, fairly high Δ_{LO-TO} values (113 and 126 cm^{-1}) are observed in the two samples obtained with the oxygen flow rates of 50 and 100 sccm, respectively. For the sake of comparison, the Δ_{LO-TO} value for v-SiO_2 is around 185 cm^{-1}.[48]

For the sample prepared without oxygen in the discharge, as shown in Table 6, the splitting of the AS1 mode is only 51 cm^{-1}. This low splitting amplitude is due to the fact that the network is not based only on oxygen bridges but also on methylene bridges, which provoke a "dilution" of Si−O−Si units within the film. Such a "dilution" causes a weakening of the long-range Coulombic interactions between the Si−O−Si oscillators, attenuating the LO−TO splitting amplitude.

From Table 6, for the O group samples, a steep rise of Δ_{LO-TO} can be seem as F_{O_2} varies from 0 to 50 sccm,

but F_{O_2} values exceeding 50 sccm promote only a small increase in Δ_{LO-TO}. An increased oxygen incorporation is accompanied by an increase in the concentration of defects in the film, as evidenced by the appearance of sylanol group-related bands (cf. Figure 3). Clearly, the defects decrease the LO−TO amplitude since they contribute to the weakening of the long-range Coulombic interaction between the Si−O−Si oscillators. The trend of the LO−TO splitting amplitude as a function of F_{O_2} for the O group samples, i.e., the sudden increase in Δ_{LO-TO} for $F_{O_2} = 50$ sccm and the leveling-off for higher F_{O_2} values, is similar to that observed in our previous investigation of films deposited from plasmas of tetramethylsilane−O_2 mixtures.[18] As in the present work, it was observed that an excess of O_2 in the chamber promoted an increase in the concentration of defects in the film.

For the samples of the N group, as shown in Table 6, the addition of N_2 in the HMDSO−He discharge attenuates the LO−TO splitting amplitudes to values even smaller than that of the He100 sample. This decrease is due to the fact that, besides oxygen and methylene bridges, there are also NH bridges, rendering the long-range interactions among Si−O−Si groups even weaker.

All these observations are very relevant since the position of the AS1 band is very steady for all samples, regardless of the deposition parameters, so that further structural information could not be drawn from its position. On the other hand, we have shown that the LO−TO splitting is very sensitive to structural characteristics of the materials under investigation. Thus, the analysis of the LO and TO functions, rather than only the original transmittance spectra, opens new perspectives on the applications of IR spectroscopy.

It is important to notice that appreciable LO−TO splittings were not observed for all bands in the IR spectra. In the high-frequency region (Figure 3), for instance, the LO and TO functions are nearly superimposed. Such a superposition may be due to a small oscillator strength or to a possible "dilution" within the solid so that they are not able to undergo long-range Coulombic interactions. It is also important to remark that the LO−TO splittings have implications on the analysis of infrared reflection−absorption spectra taken at conditions through which the Berreman effect,[50,51] can be observed, as exemplified in our previous work.[18]

Conclusions

Films of diversified structures were obtained from plasmas of HMDSO−He, HMDSO−He−O_2, and HMDSO−He−N_2. While most of our conclusions were drawn from IR data, the use of Raman spectroscopy was very useful as a complementary investigation technique, corroborating the assignments of various IR bands and revealing structures not obsevable from the IR spectra. A careful band assignment allowed the following inferences: (i) the film deposited from the HMDSO−He mixture was constituted of interconnected siloxane and carbosilane units, (ii) those deposited with oxygen in the gas feed were constituted only by interconnected siloxane units, and (iii) those deposited with nitrogen in the gas feed were similar to that obtained from the HMDSO−He mixture with the incorporation of small amounts of silazane units. Both the TO and LO spectra were obtained for all samples. It was observed that the LO−TO splitting amplitude of the asymmetrical stretching mode of Si−O in Si−O−Si groups is sensitive to the film structure, while its TO band position is not.

Acknowledgment. The Fundação de Amparo à Pesquisa do Estado de São Paulo is acknowledged for financial support (Grants 98/11743-2, 98/10979-2, and 02/07482-6) as is the Conselho Nacional de Desenvolvimento Científico e Tecnológico-CNPq. We are also indebted to Dr. Donald C. McKean for enlightening discussions about band assignments, to Dr. M. Isabel Felisberti for clarifying discussions regarding polymer terminology, to Mr. Dailto Silva for assistance in the Raman spectra acquisition, and to Donga de Souza and Dr. Lucila Cescato for refractive index measurements.

References and Notes

(1) Pryce Lewis, H. G.; Edell, D. J.; Gleason, K. K. *Chem. Mater.* **2000**, *12*, 3488.
(2) Matsuyama, H.; Kariya, A.; Teramoto, M. *J. Appl. Polym. Sci.* **1994**, *51*, 689.
(3) Magni, D.; Descheneaux, C.; Hollenstein, C.; Creatore, A.; Fayet, P. *J. Phys. D: Appl. Phys.* **2001**, *34*, 87.
(4) Furusawa, T.; Daisuke, R.; Yoneyama, R.; Homma, Y.; Hinode, K. *Electrochem. Solid-State Lett.* **2001**, *4*, G31.
(5) Wróbel, A. M.; Wertheimer, M. R.; Dib, J.; Schreiber, H. P. *J. Macromol. Sci., Chem.* **1980**, *A14*, 321.
(6) Wróbel, A. M.; Kryszewski, M.; Gazicki, M. *J. Macromol. Sci., Chem.* **1983**, *A20*, 583.
(7) Pai, P. G.; Chao, S. S.; Takagi, Y.; Lukovsky, G. *J. Vac. Sci. Technol. A* **1986**, *4*, 689.
(8) Rau, C.; Kulisch, W. *Thin Solid Films* **1994**, *249*, 28.
(9) Theil, J. A.; Brace, J. G.; Knoll, R. W. *J. Vac. Sci. Technol. A* **1994**, *12*, 1365.
(10) Da Cruz, N. C.; Durrant, S. F.; Bica de Moraes, M. A. *J. Polym. Sci., Part B: Polym. Phys.* **1998**, *36*, 1873.
(11) Hinds, B. J.; Wang, F.; Wolfe, D. M.; Hinkle, C. L.; Lucovsky, G. *J. Non-Cryst. Solids* **1998**, *227*, 507.
(12) Wolfe, D. M.; Hinds, B. J.; Wang, F.; Lucovsky, G.; Ward, B. L.; Xu, M.; Nemanich, R. J. *J. Vac. Sci. Technol. A* **1999**, *17*, 2170.
(13) Green, M. L.; Brasen, D.; Evanslutterodt, K. W.; Feldman, L. C.; Krisch, K.; Lennard, W.; Tang, H. T.; Manchanda, L.; Tang, M. T. *Appl. Phys. Lett.* **1994**, *65*, 848.
(14) Rignanese, G.-M.; Pasquarello, A.; Charlier, J.-C.; Gonze, X.; Car, R. *Phys. Rev. Lett.* **1997**, *79*, 5174.
(15) Sugahara, S.; Usami, K.; Matsumura, M. *Jpn. J. Appl. Phys.* **1999**, *38*, 1428.
(16) Sugahara, S.; Kadoya, T.; Usami, K.; Hattori, T.; Matsumura, M. *J. Electrochem. Soc.* **2001**, *148*, F120.
(17) Usami, K.; Sugahara, S.; Kadoya, T.; Matsumura, M. *Proceedings of the 7th International Sumposium on Quantum Effect Electronics;* Tokyo Institute of Technology, 2000.
(18) Trasferetti, B. C.; Davanzo, C. U.; Bica de Moraes, M. A. *J. Phys. Chem. B* **2003**, *107*, 10699.
(19) Kittel, C. *Introduction to Solid State Physics*, 7th ed.; John Wiley & Sons: New York, 1996.
(20) Blakemore, J. S. *Solid State Physics*, 2nd ed.; Cambridge Universtiy Press: Cambridge, 1995.
(21) Fleischer, H.; McKean, D. C. *J. Phys. Chem. A* **1999**, *103*, 727.
(22) McKean, D. C. *Spectrochim. Acta, Part A* **1999**, *55*, 1485.
(23) McKean, D. C.; Davidson, G.; Woodward, L. A. *Spectrochim. Acta* **1970**, *26 A*, 1815.
(24) Heavens, O. S. *Phys. Thin Films* **1964**, *2*, 120.
(25) Yamamoto, K.; Ishida, H. *Vib. Spectrosc.* **1994**, *8*, 1.
(26) Hawranek, J. P.; Jones, R. N. *Spectrochim. Acta* **1976**, *32*, 99.
(27) Ten, Y.-S.; Wong, J. S. *J. Phys. Chem.* **1989**, *93*, 7208.
(28) McKean, D. C. Personal communication.
(29) Marchand, A.; Valade, J.; Forel, M.-T.; Josien, M.-L.; Calas, R. *J. Chim. Phys.* **1962**, *59*, 1142.
(30) Anderson, D. R. In *Analysis of Silicones*; Smith, A. L., Eds.; John Wiley & Sons: New York, 1974.
(31) Lee Smith, A.; Anderson, D. R. *Appl. Spectrosc.* **1984**, *38*, 822.
(32) Bellamy, L. J. *The Infra-Red Spectra of Complex Molecules;* Chapman & Hall: London, 1975.
(33) Kirk, C. T. *Phys. Rev. B* **1988**, *38*, 1255.
(34) Pasquarello, A.; Car, R. *Phys. Rev. Lett.* **1997**, *79*, 1766.

(35) Calzaferri, G.; Imhof, R.; Törnroos, K. W. *J. Chem. Soc., Dalton Trans.* **1994**, 3123.
(36) Marcolli, C.; Calzaferri, G. *Appl. Organomet. Chem.* **1999**, *13*, 213.
(37) Pryce Lewis, H. G.; Casserly, T. B.; Gleason, K. K. *J. Electrochem. Soc.* **2001**, *148*, F212.
(38) Ono, H.; Ikarashi, T.; Miura, Y.; Hasegawa, E.; Ando, K.; Kitano, T. *Appl. Phys. Lett.* **1999**, *74*, 203.
(39) Scarlete, M.; Brienne, S.; Butler, I. S.; Harrod, J. F. *Chem. Mater.* **1994**, *6*, 977.
(40) Tsu, D. V.; Lucovsky, G.; Davidson, B. N. *Phys. Rev. B* **1989**, *40*, 1795.
(41) Inagaki, N.; Koyama, M. *J. Appl. Polym. Chem. Ed.* **1983**, *21*, 1847.
(42) Alexander, M. R.; Jones, F. R.; Short, R. D. *J. Phys. Chem. B* **1997**, *101*, 3614.
(43) Theirich, D.; Soll, C.; Leu, F.; Engemann, J. *Vacuum* **2003**, *71*, 348.
(44) Pryce Lewis, H. G.; Edell, D. J.; Gleason, K. K. *Chem. Mater.* **2000**, *12*, 3488.
(45) Guiton, T. A.; Pantano, C. G. *Colloids Surf., A* **1993**, *74*, 33.
(46) Kamitsos, E. I.; Patsis, A. P.; Kordas, G. *Phys. Rev. B* **1993**, *48*, 12499.
(47) Sarnthein, J.; Pasquarello, A.; Car, R. *Science* **1997**, *275*, 1925.
(48) Trasferetti, B. C.; Davanzo, C. U. *Appl. Spectrosc.* **2000**, *54*, 502.
(49) LO−TO splittings are related to the dipole moment derivative through the following equation: $\nu_{LO}^2 - \nu_{TO}^2 = (N/\pi c^2)[(n_\infty + 2)/3n_\infty]^2(\partial\mu/\partial q)^2$. In this expression n_∞ is the refractive index at high frequency, N is is the number of molecules/cm^3, and $\partial\mu/\partial q$ is the derivative of the dipole moment with respect to the normal coordinate for ν_0 ($0 \rightarrow 1$), which is the frequency of the oscillator "expected in the absence of the long-range, electrostatic coupling" [see: Decius, J. C. *J. Chem. Phys.* **1968**, *49*, 1387 and ref 45].
(50) Berreman, D. W. *Phys. Rev.* **1963**, *130*, 2193.
(51) Jones, L. H.; Swanson, B. I. *J. Phys. Chem.* **1991**, *95*, 2701.

MA035297A